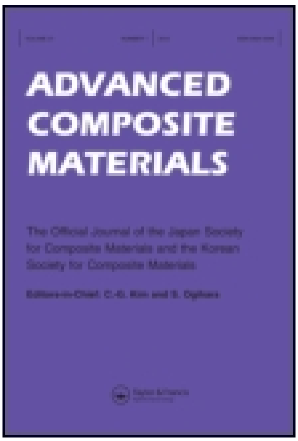

Advanced Composite Materials
Publication details, including instructions for authors and subscription information:
http://www.tandfonline.com/loi/tacm20

Interaction of shear wave with fiber orientations in composite laminate: model and experiment

David K. Hsu & Dong Fei

Version of record first published: 02 Apr 2012.

To cite this article: David K. Hsu & Dong Fei (2002): Interaction of shear wave with fiber orientations in composite laminate: model and experiment , Advanced Composite Materials, 11:1, 61-69

To link to this article: http://dx.doi.org/10.1163/156855102753613291

Adv. Composite Mater., Vol. 11, No. 1, pp. 61–69 (2002)

Interaction of shear wave with fiber orientations in composite laminate: model and experiment

DAVID K. HSU * and DONG FEI

Center for Nondestructive Evaluation, 133 ASC II, 1915 Scholl Road, Iowa State University, Ames, IA 50011-3042, USA

Abstract—Linearly polarized transverse (shear) waves propagating in the thickness direction of a composite laminate interact strongly with the fiber directions in the discrete plies of the laminate. Shear waves transmitted through or reflected from a laminate therefore contain information about its stacking sequence and layup orientation. In the case of transmission, one can also exploit the analogy with the polarizer-analyzer configuration in optics. It has been shown that the interaction between shear waves and fiber directions can lead to high sensitivity for the detection of certain errors in the layup or stacking sequence of a laminate. This paper describes a complete analytical model for the propagation of shear waves in a laminate using local and global transfer matrices. Transmitted and reflected signal amplitude as a function of angle and time (or frequency) can be predicted for a given input. Experimental results are also shown for a transmission setup that uses electromagnetic acoustic transducers (EMATs) for the generation and reception of normal incidence shear waves in cured and uncured composite laminates.

Keywords: Shear waves; ply layup errors; composite laminates.

1. INTRODUCTION

Due to the highly anisotropic elastic properties of the plies in a fiber-reinforced composite laminate, transverse (shear) waves propagated through the laminate, or reflected from its back surface, carry rich information about the fiber orientation and ply stacking sequence in the laminate. Such signals can therefore be used in the nondestructive detection of ply layup or stacking sequence errors in composite laminates. Some attempts have been reported for exploiting the strong interaction between shear wave polarization and fiber orientation for nondestructive evaluation (NDE) purposes [1–4]. For example, Hsu *et al.* [2–4] have used the 'crossed polarizer' configuration in which the transmitting and receiving transducers on the

*To whom correspondence should be addressed. E-mail: dhsu@cnde.iastate.edu

two faces of the laminate were perpendicular to each other and both were rotated in unison over a full circle. The transmitted signal was found to have good sensitivity for certain ply orientation and stacking sequence anomalies. However, it is not until recently that a complete analytical model was developed by Fei and Hsu [5–7] for the propagation of shear waves in composite laminates and verified by a series of experiments. The analytical model led to a result that is very compact and tractable. The four transfer functions F_{ij} $(i, j = 1, 2)$ that contain the most information can be determined experimentally for a given laminate by four measurements, with the transmitter angle and receiver angle at (0, 0), (0, 90), (90, 0), and (90, 90). The model takes into account all the reflected waves at the interfaces in the laminate by including the four partial waves in each layer that are polarized parallel to and perpendicular to the fiber, and propagating in the forward and reversed directions. The model for the transmission geometry has been experimentally verified using both cured and uncured laminates; it has now been extended to the case of reflection (pulse-echo).

An experimental problem with making reproducible shear wave measurements has been the need for a shear wave couplant. Keeping the coupling condition constant has been especially problematic for measurements that require frequent change of the angular orientation of the shear wave transducers. To alleviate this problem, researchers at Iowa State University used EMAT probes for the generation and detection of normal incidence shear waves in a non-contact manner. The composite sample was sandwiched between two aluminum blocks and the EMAT probes were placed on the outside faces of the two blocks. The EMATs can be rotated freely with computer-controlled stepping motors in an angular scan. For uncured laminates, the pressure applied on the blocks was sufficient for shear waves to transmit through. For solid cured laminates, shear couplant was still used between its surfaces and the aluminum; however, the coupling condition was not disturbed by rotation and hence remained constant. The analytical model was used to predict the transmitted signals for a number of laminate layup with various likely ply orientation errors and stacking sequence anomalies. The comparison of model and experimental results for selected cases is presented in this paper.

2. MODELING

An idealized layered model, shown in Fig. 1b, has been established to model the EMAT-generated shear wave transmission measurement shown in Fig. 1a. The EMAT transmitter and receiver are modeled as linearly polarized plane shear wave generator and receiver, respectively. The aluminum blocks are modeled as two isotropic half spaces and the composite is modeled as a material structure that contains many plies, each of which is modeled as a homogeneous transversely-isotropic material with the plane of isotropy normal to the fiber direction. All the boundaries, including the ply–ply interfaces within the laminate and the

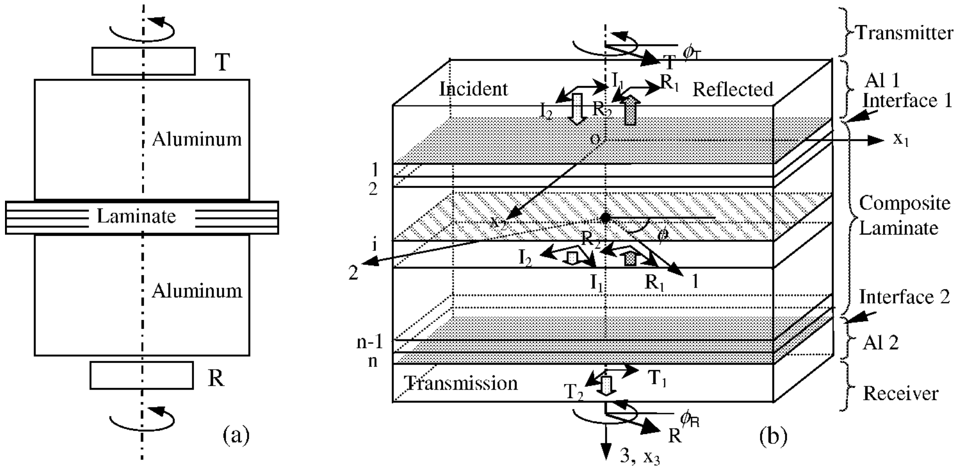

Figure 1. Model idealization. (a) measurement configuration; (b) model.

aluminum–laminate interfaces, are assumed to be perfect so that the continuity conditions of displacement (or velocity) and stress can be applied.

To model the transmission output, we express the shear wave field in each ply as a summation of four partial wave fields: two fast shear waves propagating up and down, and two slow shear waves propagating up and down. Then we use the velocity and stress continuity conditions at each interface, including ply interfaces in the sample and sample–aluminum interfaces, to set up and solve the equations for the unknown transmission fields. Velocity continuity conditions, instead of displacement continuity conditions, are used so that the final equation can be expressed in terms of acoustic impedance, which is more compact and physically meaningful. The transfer matrix technique [8] is used to simplify the above solution process. But instead of using the transfer matrix directly, we use an inverse transfer matrix to simplify the final expression. A brief description of the derivation process is given below. A more complete description can be found in [7].

2.1. Shear wave generation and detection

As shown in Fig. 1b, using the linear polarization assumption, the two displacement components of the incident shear wave can be expressed as

$$\begin{bmatrix} I_1 \\ I_2 \end{bmatrix}^{+}_{\mathrm{Al}_1} = V_i \beta_{\mathrm{T}}(\omega) \begin{bmatrix} \cos\phi_{\mathrm{T}} \\ \sin\phi_{\mathrm{T}} \end{bmatrix}, \tag{1}$$

where I_1 and I_2 are the displacement components of the incident shear wave, V_i is the source voltage, ω is angular frequency, $\beta_{\mathrm{T}}(\omega)$ is the efficiency factor for the transmitter, and ϕ_{T} is the polarization direction of the transmitter. For detection in the transmission mode, we have

$$V_o = \beta_R(\omega) [\, T_1 \quad T_2 \,] \begin{bmatrix} \cos\phi_R \\ \sin\phi_R \end{bmatrix}, \tag{2}$$

where T_1 and T_2 are the displacement components of the transmitted shear wave, V_o is the output voltage, $\beta_R(\omega)$ is the efficiency factor for the receiver side, and ϕ_R is the polarization direction of the receiver.

2.2. Transfer functions

By applying the velocity and stress continuity conditions at each interface in the sample, we can relate the velocity-stress vectors at the top and bottom interfaces of the whole sample by a global inverse transfer matrix B, as follows,

$$P^-_{\text{sample}} = B P^+_{\text{sample}}, \tag{3}$$

where velocity-stress vector $P(= [\, v_1 \quad v_2 \quad \sigma_{13} \quad \sigma_{23} \,]^{\mathrm{T}})$ contains the velocity and stress components associated with the shear wave field, and $B(= B_1 B_2 \ldots B_{n-1} B_n)$ is a product of the local inverse transfer matrices $B_i (i = 1, 2, \ldots, n)$ whose detailed expressions are given in [7].

In aluminum medium 1, the velocity-stress vector at interface 1 can be expressed as

$$P^+_{\mathrm{Al}_1} = (-i\omega) \begin{bmatrix} 1 & 0 & 1 & 0 \\ 0 & 1 & 0 & 1 \\ -Z & 0 & Z & 0 \\ 0 & -Z & 0 & Z \end{bmatrix}_{\mathrm{Al}_1} \begin{bmatrix} I_1 \\ I_2 \\ R_1 \\ R_2 \end{bmatrix}_{\mathrm{Al}_1}, \tag{4}$$

where Z is the acoustic impedance of the shear wave in aluminum, R_1 and R_2 are the displacement components of the reflected shear wave, respectively. In medium 2, there are only two transmitted partial waves and the velocity-stress vector at the top interface is given by,

$$P^-_{\mathrm{Al}_2} = (-i\omega) \begin{bmatrix} 1 & 0 \\ 0 & 1 \\ -Z & 0 \\ 0 & -Z \end{bmatrix}_{\mathrm{Al}_2} \begin{bmatrix} T_1 \\ T_2 \end{bmatrix}_{\mathrm{Al}_2}. \tag{5}$$

Combining equations (3), (4) and (5) and applying velocity-stress continuity conditions at the two aluminum-sample interfaces, we can set up the equations for the unknown reflected and transmitted components in aluminum media. Solving the equations, we get the transmitted components T_1 and T_2 in the form of

$$\begin{bmatrix} T_1 \\ T_2 \end{bmatrix} = \begin{bmatrix} F_{11} & F_{12} \\ F_{21} & F_{22} \end{bmatrix} \begin{bmatrix} I_1 \\ I_2 \end{bmatrix}, \tag{6}$$

where $F_{ij}(i, j = 1, 2)$ are the transfer functions that relate the arbitrary incident inputs with the transmission outputs. The detailed expressions for F'_{ij}s can be found in [7].

2.3. Output voltage

The expression for the output voltage can be obtained by combining equations (1), (2) and (6), which leads to

$$V_o = V_i \beta_T(\omega)\beta_R(\omega) \left[\cos\phi_R \quad \sin\phi_R \right] \begin{bmatrix} F_{11} & F_{12} \\ F_{21} & F_{22} \end{bmatrix} \begin{bmatrix} \cos\phi_T \\ \sin\phi_T \end{bmatrix}. \tag{7}$$

From equation (7), we can see that the layup information is contained in the transfer functions, and therefore there is no simple relationship between the transmission output and the layup. We can, however, detect the layup error by changing the frequency and the orientation of the transducers and monitoring the output accordingly. In essence, the transfer functions contain the maximum information that can be obtained from the transmission or reflection measurement. These transfer functions can be determined in principle by just four measurements: with (1) $\phi_T = \phi_R = 0°$; (2) $\phi_T = \phi_R = 90°$; (3) $\phi_T = 0°$, $\phi_R = 90°$; and (4) $\phi_T = 90°$, $\phi_R = 0°$, respectively.

2.4. Angular scan patterns

It has been found that the angle-frequency patterns (transmission spectra at different angles), for either 'aligned' (where the EMATs are parallel to each other during an angular scan) or 'crossed' (where the EMATs are normal to each other during an angular scan) configurations, are very sensitive to layup errors [6, 7]. Figure 2 shows the modeled crossed angle-frequency patterns for a cross-ply graphite/epoxy laminate with and without stacking sequence errors. It can be seen that the changes of pattern due to layup errors are very obvious. Extensive model calculations for other types of laminates with other types of layup errors also show that the angle-frequency patterns or the equivalent angle-time patterns (transmission waveforms at different angles) are very sensitive to layup errors.

2.5. Reflection method

Compared to the transmission method, the reflection method has a big advantage of single-side access. To model the reflection output, the same procedure as the above

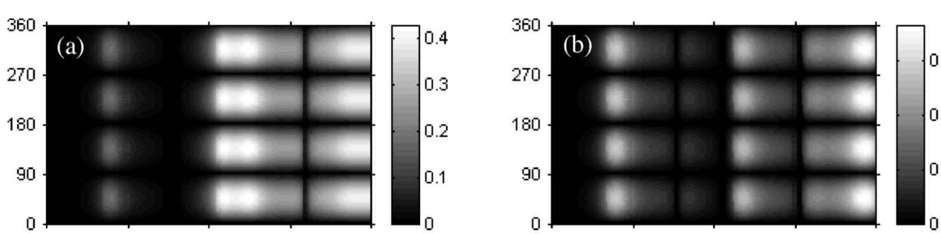

Figure 2. Modeled crossed angle-frequency patterns for graphite/epoxy laminates with and without errors. Layup: $[(0/90)]_{2S}$. (a) without error; (b) crossed, plies 2 and 3 are exchanged. For all patterns, the horizontal axis is frequency in MHz and the vertical axis is angle of the transmitter in degrees.

can be used. Referring to Fig. 1, since there is no separate receiving transducer and the associated aluminum block necessary in a transmission measurement, interface 2 is traction free. Using equations (3) and (4) and the velocity-stress continuity condition at interface 1, we can again set up the equations and solve the unknown reflected fields R_1 and R_2. Similar to equation (6), we have

$$\begin{bmatrix} R_1 \\ R_2 \end{bmatrix} = \begin{bmatrix} H_{11} & H_{12} \\ H_{21} & H_{22} \end{bmatrix} \begin{bmatrix} I_1 \\ I_2 \end{bmatrix}, \tag{8}$$

where H contains the first two rows and columns of a matrix X, which is given by

$$X = \begin{bmatrix} 1 & 0 & -B_{11} & -B_{12} \\ 0 & 1 & -B_{21} & -B_{22} \\ Z & 0 & -B_{31} & -B_{32} \\ 0 & Z & -B_{41} & -B_{42} \end{bmatrix}^{-1} \begin{bmatrix} -1 & 0 \\ 0 & -1 \\ Z & 0 \\ 0 & Z \end{bmatrix}. \tag{9}$$

The above expression can be further simplified using symbolic evaluation. Using equation (8) and the linear polarization assumption of the shear wave generation and detection, we can also get the expression for the reflected output, which is just equation (7) with ϕ_{T} and F respectively replaced by ϕ_{R} and H.

3. EXPERIMENTAL

An azimuthal EMAT scan system [5, 6] has been developed for experimental verification of the model. In the scan system, the composite sample is sandwiched between two aluminum blocks. For cured composite laminates, a shear couplant was used at the composite–metal interfaces. In the case of uncured laminates, no couplant is needed and the shear wave can be detected effectively via the pressure applied on the sample. Two stepper motors, controlled by a computer through a motor driver, are used to rotate the EMATs (with a central frequency of about 1.3 MHz and a bandwidth of about 1 MHz) simultaneously. The EMAT transmitter is driven by a burst pulser (RITEC BP-9400). The transmitted signals, after being amplified and filtered, are acquired by the computer for further analysis. The azimuthal scan can be either ‘aligned’ or ‘crossed’. Under computer control, a typical azimuthal scan can be done in about 3 minutes.

4. RESULTS AND DISCUSSION

The first case studied is a 24-ply unidirectional graphite/epoxy laminate. Figures 3a and 3b show the experimental and model-predicted crossed angle-time patterns, respectively. The angle-time pattern shows a 2D plot of the transmission waveforms obtained at different angular positions of EMATs during the scan. The time-domain model prediction is generated by calculating the spectrum of the reference signal obtained with the two aluminum blocks coupled directly together by couplant,

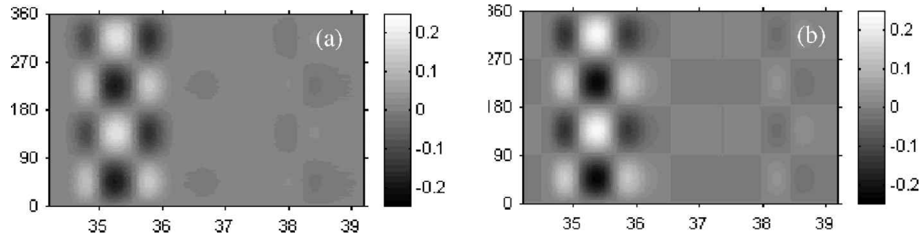

Figure 3. Angle-time patterns for a 24-ply unidirectional graphite/epoxy laminate: (a) experimental; (b) model. For all patterns, the horizontal axis is time in μs and the vertical axis is angle of the transmitter in degrees.

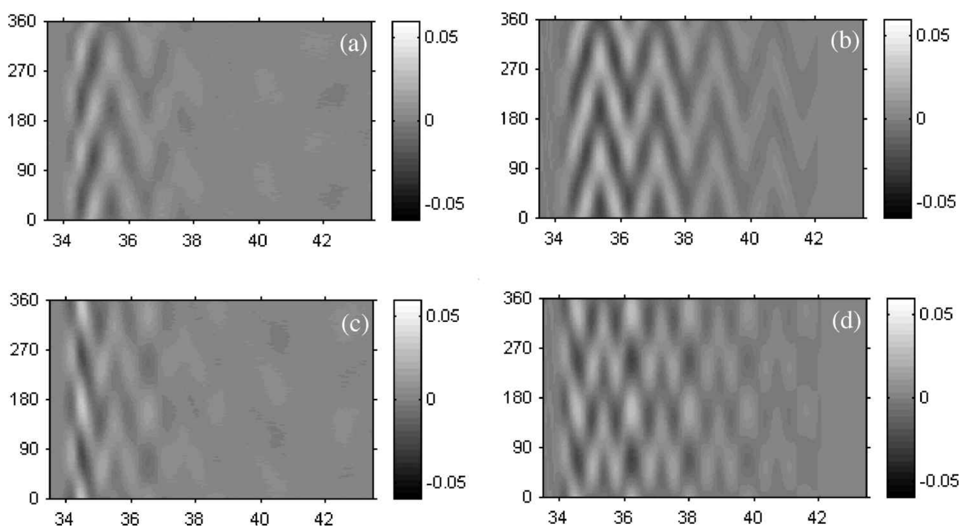

Figure 4. Crossed angle-time patterns for uncured graphite/epoxy laminates with and without layup errors. Layup:$[(0/45/90/-45)]_S$. (a) without error, experimental; (b) without error, model; (c) with ply 4 at 45°, experimental; (d) with ply 4 at 45°, model. For all patterns, the horizontal axis is time in μs and the vertical axis is angle in degrees for the transmitter.

multiplying the result by the transmission coefficient and transforming back into the time domain. It could be seen that the experimental results and the model prediction agree with each other very well. The aligned results are equally good.

The second example is a case of an 8-ply uncured quasi-isotropic graphite/epoxy laminate. Figures 4a and 4b show the experimental pattern for the crossed configuration and its model prediction for the sample free of layup errors, respectively. We can see that the model predicted the main features of the experimental pattern. In the experimental pattern, the signal decays faster than the model prediction because of the high attenuation of the uncured laminate, which is not included in the model. Figures 4c and 4d show the crossed experimental pattern and its model prediction for the sample with the 4th ply misplaced at +45°. By comparison, we can see that the changes of the pattern due to the fiber misorientation are very obvious, and that the model predicated such changes of the pattern fairly well. Experiments performed on other laminate layups in the model validations were similarly successful.

5. CONCLUSIONS

By developing an analytical model and conducting experimental verification, we have established normally incident shear waves as a quantitative NDE method for the evaluation of composite laminates. The use of EMATs has made it possible to have a computerized angular scan and data acquisition system for transmitted shear waves. The amplitude patterns of the transmitted signal, displayed as a function of time and angle (or frequency and angle), contain distinct features that reflect certain properties of the laminate. The experimental validation of the analytical model in cured and uncured composite laminates has been largely successful. Together with the computerized EMAT angular scan system, the analytical model continues to serve as a useful tool for the nondestructive detection of manufacturing anomalies in composite laminates.

Acknowledgements

This work was supported by the NSF Industry/University Cooperative Research Center for Nondestructive Evaluation at Iowa State University. One of the authors (D. Fei) acknowledges the support of a fellowship from the Institute for Physical Research and Technology at Iowa State University.

REFERENCES

1. I. N. Komsky, I. M. Daniel and Y. C. Yee, Ultrasonic determination of layer orientation in multi-layer multi-directional composite laminates, in: *Rev. of Prog. in Quantitative NDE*, D. O. Thompson and D. E. Chimenti (Eds), Vol. 11, pp. 1615–1622. Plenum Press, New York (1992).
2. D. K. Hsu and F. J. Margetan, Examining CFRP laminate layup with contact-mode ultrasonic measurement, *Adv. Comp. Lett.* **2** (2), 51–54 (1993).
3. B. A. Fischer and D. K. Hsu, Application of shear waves for composite laminate characterization, in: *Rev. of Prog. in Quantitative NDE*, D. O. Thompson and D. E. Chimenti (Eds), Vol. 15, pp. 1191–1198. Plenum Press, New York (1996).
4. D. K. Hsu, B. A. Fischer and M. Koskamp, Shear wave ultrasonic technique as an NDE tool for composite laminate before and after curing, in: *Rev. of Prog. in Quantitative NDE*, D. O. Thompson and D. E. Chimenti (Eds), Vol. 16, pp. 1975–1982. Plenum Press, New York (1997).
5. D. Fei and D. K. Hsu, Development of motorized azimuthal scanners for ultrasonic NDE of composites, in: *Rev. of Prog. in Quantitative NDE*, D. O. Thompson and D. E. Chimenti (Eds), Vol. 18, pp. 1385–1392. Kluwer Academic/Plenum Publishers, New York (1999).
6. D. Fei and D. K. Hsu, EMAT-generated shear wave transmission for NDE of Composite laminates, in: *Rev. of Prog. in Quantitative NDE*, D. O. Thompson and D. E. Chimenti (Eds), Vol. 19, pp. 1159–1166. American Institute of Physics, Melville, NY (2000).

7. D. K. Hsu and D. Fei, EMAT-generated shear waves as a probe for composite laminate layup errors, in: *Proceedings of the 45th International SAMPE Symposium*, Long Beach, CA, pp. 1670–1681 (2000).
8. A. H. Nayfeh, *Wave Propagation in Layered Anisotropic Media with Applications to Composites.* Elsevier Science, Amsterdam, New York (1995).